

Intraband exciton relaxation in a biased lattice with long-range correlated disorder

E. Díaz and F. Domínguez-Adame

GISC, Departamento de Física de Materiales, Universidad Complutense, E-28040 Madrid, Spain

We study numerically the intraband exciton relaxation in a one-dimensional lattice with scale-free disorder, in the presence of a linear bias. Exciton transport is considered as incoherent hoppings over the eigenstates of the static lattice. The site potential of the unbiased lattice is long-range-correlated with a power-law spectral density $S(k) \sim 1/k^\alpha$, $\alpha > 0$. The lattice supports a phase of extended states at the center of the band, provided α is larger than a critical value α_c [F. A. B. F. de Moura and M. L. Lyra, *Phys. Rev. Lett.* **81**, 3735 (1998)]. When the bias is applied, the absorption spectrum displays clear signatures of the Wannier-Stark ladder [E. Díaz *et al.*, *Phys. Rev. B* **73**, 172410 (2006)]. We demonstrate that in unbiased lattices and in weakly correlated potentials the decay law is non-exponential. However, the decay is purely exponential when the bias increases and α is large. We relate this exponential decay to the occurrence of the Wannier-Stark ladder in the exciton band.

PACS numbers: 32.50.+d; 71.35.Aa; 78.30.Ly

I. INTRODUCTION

Long-range correlations with spectral density of the form $S(k) \sim 1/k^\alpha$ often arise in nature.^{1,2} It has been argued that long-range correlations in nucleotide sequences can explain the long-distance charge transport in DNA.^{3,4,5,6} This type of correlations may result in a phase of extended states at the center of the band, provided α is larger than a critical value α_c .⁷ Therefore, a localization-delocalization transition at the two mobility edges, separating the phase of extended states at the band center from the localized ones at the band tails, is found in these systems.^{8,9} It was demonstrated later that $\alpha_c = 2$ is the universal critical value for the localization-delocalization transition to occur in the model introduced in Ref. 7, independently of the magnitude of disorder.¹⁰

Bloch-like oscillations¹¹ of quasiparticles are known to arise in biased one-dimensional (1D) systems with $S(k) \sim 1/k^\alpha$ spectral density.¹² These oscillations provide a way to measure the energy width of the delocalized phase since it determines the amplitude of the oscillations. In addition, the frequency-domain counterpart of the Bloch oscillations, the so-called Wannier-Stark ladder (WSL),¹³ was also observed in the optical absorption spectrum, in spite of the underlying randomness.¹⁴ Strong correlations in the disorder facilitate the observation of the WSL. At $\alpha > \alpha_c$, when the phase of extended states emerges at the center of the band, a periodic series of identical peaks is found to build up at the center of the absorption band. This periodic pattern was related to the Wannier-Stark quantization of the energy spectrum in the disordered lattice.¹⁴

In this work we report further progress along this line. We present a model Hamiltonian for excitons interacting with vibrations of the host medium. We assume that there exists an intrinsic bias affecting the exciton dynamics, as occurs in dendrimers for instance.¹⁵ Furthermore, site energies are assumed to be long-range correlated with $S(k) \sim 1/k^\alpha$ spectral density. The aim of this work is twofold. First, we analyze how intraband relaxation,

due to the coupling to the vibrations of the glassy host medium, affects the time behavior of the exciton decay in the *biased* lattice. Second, we look for signatures of the WSL in the radiative decay of excitons.

The outline of the paper is as follows. In the next section we present our model, which is based on a tight-binding Hamiltonian of an exciton in a long-range-correlated potential landscape and subjected to a linear bias. In Sec. III we recall the basic physics of the exciton intraband relaxation due to the coupling to host vibrations. Exciton dynamics will be described by a Pauli master equation for the populations of the exciton states.¹⁶ The central part of the paper are Secs. IV and V, where we present the results of numerical simulations of the time decay of fluorescence after broadband pulse excitation in disorder-correlated systems. We discuss in detail its dependence on the driving parameters of the model (bias magnitude, disorder strength and correlation exponent α) and provide an evidence of that the WSL reveals in the intraband exciton relaxation. We find that the fluorescence decay exponentially when localization by the bias prevails over localization by disorder. We relate this exponential decay to the occurrence of the WSL. When disorder is large enough or long-range correlations are weak ($\alpha < \alpha_c$), the time dependence of the fluorescence decay is non-exponential. Finite size effects on the time decay of fluorescence are analyzed in Sec. VI. Finally, Sec. VII concludes the paper.

II. MODEL HAMILTONIAN

We consider a biased tight-binding model with diagonal disorder on an otherwise regular 1D open lattice of spacing unity and N sites (N is assumed to be even). We assign two levels to each lattice site, ground and excited, and consider optical transitions between them with transition energy $\mathcal{E}_n = \bar{\mathcal{E}} + \varepsilon_n$. The stochastic part ε_n is

generated according to⁷

$$\varepsilon_n = \sigma C_\alpha \sum_{k=1}^{N/2} \frac{1}{k^{\alpha/2}} \cos\left(\frac{2\pi kn}{N} + \phi_k\right), \quad (1a)$$

where the normalization constant is given by

$$C_\alpha = \sqrt{2} \left(\sum_{k=1}^{N/2} \frac{1}{k^\alpha} \right)^{-1/2}. \quad (1b)$$

Here $\phi_1, \dots, \phi_{N/2}$ are uncorrelated random phases uniformly distributed within the interval $[0, 2\pi]$. The distribution (1) has zero mean $\langle \varepsilon_n \rangle = 0$ and standard deviation $\langle \varepsilon_n^2 \rangle^{1/2} = \sigma$, where $\langle \dots \rangle$ indicates averaging over realizations of random phases ϕ_k . The quantity σ will be referred to as magnitude of disorder.

The model Hamiltonian is

$$\begin{aligned} \mathcal{H} = & \sum_{n=1}^N \left[\varepsilon_n - U \left(n - \frac{N}{2} \right) \right] |n\rangle\langle n| \\ & - J \sum_{n=1}^{N-1} \left(|n\rangle\langle n+1| + |n+1\rangle\langle n| \right). \end{aligned} \quad (2)$$

Here, $|n\rangle$ denotes the state in which the n th site is excited, whereas all the other sites are in the ground state. The term $-U(n - N/2)$ describes the linear bias. The intersite transfer integrals in (2) are restricted to nearest-neighbors, and it is set to $-J$ over the entire lattice. Also, we set $\bar{\mathcal{E}} = 0$ hereafter without loss of generality.

As we already mentioned in Sec. I, the unbiased model supports a phase of extended states at the center of the band, provided the correlation exponent α is larger than a critical value α_c . On the contrary, all the states are localized at $\alpha < \alpha_c$.

III. INTRABAND RELAXATION

Excitons can hop between the eigenstates of the Hamiltonian (2) only if coupling to vibrations is taken into account. We assume that this coupling is weak and do not consider polaron effects. The exciton-vibration interaction causes the *incoherent* hopping of excitons from one eigenstate to another. Only one-phonon processes are considered throughout the paper. We take the transition rate from the state ψ_μ (with energy E_μ) to the state ψ_ν (with energy E_ν) according to (see Ref. 16 for further details)

$$W_{\mu\nu} = W_0 S(|\Delta E_{\mu\nu}|) F(\Delta E_{\mu\nu}, T) \mathcal{I}_{\mu\nu}, \quad (3)$$

with $\Delta E_{\mu\nu} \equiv E_\mu - E_\nu$. The constant W_0 characterizes the amplitude of transitions. A spectral density function of the form $S(|\Delta E|) = |\Delta E|/J$ holds for glassy hosts.^{17,18} Temperature T enters into this expression through the function $F(\Delta E, T) = \theta(-\Delta E) + n(\Delta E, T)$,

where θ is the Heaviside step function and $n(\Delta E, T) = [\exp(\Delta E/k_B T) - 1]^{-1}$ is the occupation number of the vibration mode with frequency $\Delta E/\hbar$. The parameter

$$\mathcal{I}_{\mu\nu} \equiv \sum_{n=1}^N \psi_{\mu,n}^2 \psi_{\nu,n}^2 \quad (4)$$

represents the overlap integral of exciton probabilities for the states ψ_μ and ψ_ν . Notice that the transition rates meet the principle of detailed balance: $W_{\nu\mu} = W_{\mu\nu} \exp(\Delta E_{\mu\nu}/k_B T)$.

We describe the process of exciton relaxation by means of the Pauli master equation for the level population P_μ of the μ th exciton eigenstate

$$\frac{dP_\mu}{dt} = -\gamma_\mu P_\mu + \sum_{\nu=1}^N (W_{\mu\nu} P_\nu - W_{\nu\mu} P_\mu), \quad (5)$$

where $\gamma_\nu = \gamma f_\mu$ is the spontaneous emission rate of the μ th exciton state, while γ is that of a monomer, $f_\mu = (\sum_{n=1}^N \psi_{\mu,n})^2$ being the dimensionless oscillator strength. After broadband pulse excitation, each level is populated according to its oscillator strength, namely $P_\mu(0) = f_\mu/N$. Consequently, the initial total population is normalized to unity, $\sum_\mu P_\mu(0) = 1$. The normalized fluorescence after pulse excitation is obtained from

$$I(t) = N \frac{\sum_{\mu=1}^N f_\mu P_\mu(t)}{\sum_{\mu=1}^N f_\mu^2}, \quad (6)$$

which is the magnitude of interest in this work.

IV. UNBIASED SYSTEM

We first discuss the exciton decay of the unbiased system ($U = 0$), aiming to separate the effects of bias from those related to the disordered nature of the model. We have numerically diagonalized the Hamiltonian (2) by means of standard methods and obtained the eigenstates ψ_μ and eigenvalues E_μ for different values of the correlation exponent α and magnitude of disorder σ , considering open linear lattices. In Fig. 1 we show a subset of eigenstates obtained for a typical random realization of the potential landscape for $\alpha = 4$, larger than the critical value $\alpha_c = 2$. The baselines display the corresponding eigenenergies. The lowest state in Fig. 1 (labeled 1) shows a bell-like shape and carries a large oscillator strength. There are several states of such type (not shown in Fig. 1), which are close in energy to the state 1 and do not overlap with each other. On increasing the energy, one observes eigenstates, like the one labeled 2 in Fig. 1, which are more extended, as compared to the lowest one, and present several nodes within the localization segment. The oscillator strength of such states is much smaller (dark states). Remarkably, going further up in energy we again find bell-like states, as the one labeled

3 in Fig. 1, which are characterized by a large oscillator strength. Finally, on approaching the center of the band one expects the occurrence of extended states. The state 4 in Fig. 1 represents an example.

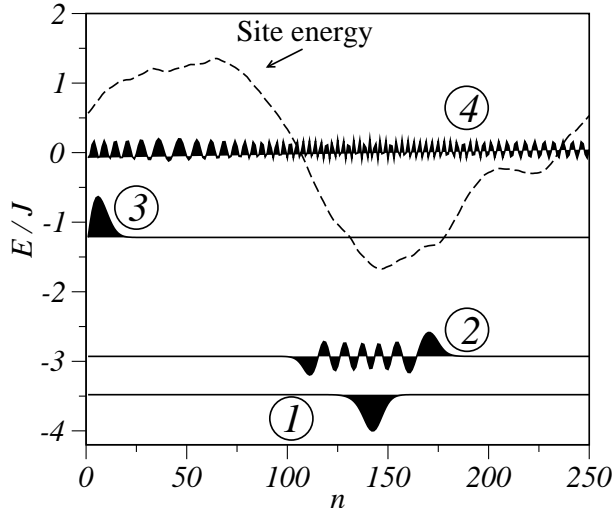


FIG. 1: A subset of eigenstates for a typical realization of the random energy potential (dashed line), for a lattice of size $N = 250$, magnitude of disorder $\sigma = J$, and correlation exponent $\alpha = 4$ (larger than the critical value $\alpha_c = 2$). The baseline indicates the energy of the eigenstate. The states 1 and 3 are those which larger oscillator strength.

The picture presented above is different when α is smaller than the critical value $\alpha_c = 2$. The level structure is then similar to what it is found in the standard 1D Anderson model (uncorrelated disorder). Bell-like states lay at the bottom of the band and dark states, localized over larger segments, are higher in energy (see, e.g., Fig. 1 in Ref. 19). In addition, there are not extended states like that labeled 4 in Fig. 1 at $\alpha < \alpha_c$.

Having in mind the different level structure for α larger and smaller than the critical value α_c , we obtained the normalized fluorescence after pulse excitation (6). Hereafter we restrict ourselves to $T = 0$; we have checked that our main conclusions are valid when the temperature is a fraction of J/k_B . This can be understood from the large energy difference between states 1 and 3 in Fig. 1, which are those strongly coupled to the light due to their high oscillator strength. In other words, it is highly improbable that an initial excitation of the state 1 can be transferred to the state 3 after several hops, at least at low T . Also, we choose the parameter $W_0 = \gamma$ hereafter, so that radiative decay is favored with respect to intraband relaxation. This statement can be understood from previous estimations in unbiased lattices with uncorrelated disorder.²⁰ When $\sigma = J$, the largest intraband transition rate $W_{\mu\nu}$ is of the order $\sim 0.06W_0$ but the higher spontaneous emission rate γ_μ is about $\sim 9\gamma$.

Figure 2 shows the fluorescence decay after pulse excitation as a function of γt for various set parameters and $W_0 = \gamma$. The lattice size is $N = 250$ and the results

comprises the average over 200 realizations of the disorder. In all cases the decay is clearly non-exponential. At large times the decay law fits well a stretched exponential $I(t) \sim \exp[-(t/\tau_\infty)^\beta]$, where both τ_∞ and $\beta < 1$ depend on the correlation exponent α . The fluorescence curves are similar when the magnitude of disorder σ is small, as can be seen in Fig. 2. However, on increasing the magnitude of disorder the fluorescence decay is slower in strongly correlated systems.

The slowing down of the fluorescence decay can be understood as follows. When α is smaller than α_c , high energy states are weakly coupled to the light due to their low oscillator strength. The excitation is then transferred from the high energy states (dark states) to those at the bottom of the band (bell-like states). Being stuck in the bottom state, the exciton emits a photon on average after a time $1/\gamma_1$ has elapsed. On the contrary, when α is larger than α_c , the initial exciton population does not decrease monotonously on increasing energy due to occurrence of bell-like states like that labeled 3 in Fig. 1 (recall that the initial level population is proportional to the corresponding oscillator strength). In contrast to bell-like states at the bottom of the band, those highly populated states after excitation may not decay radiatively: an exciton initially located at state 3 in Fig. 1 may be transferred to a state of lower energy whose oscillator strength is vanishingly small (e.g. state 2 in Fig. 1). The exciton is then scattered to bottom states (e.g. state 1 in Fig. 1) and then emits a photon. Consequently, on average there are more intraband scattering events through dark states when α is large, yielding a slowdown observed in Fig. 2.

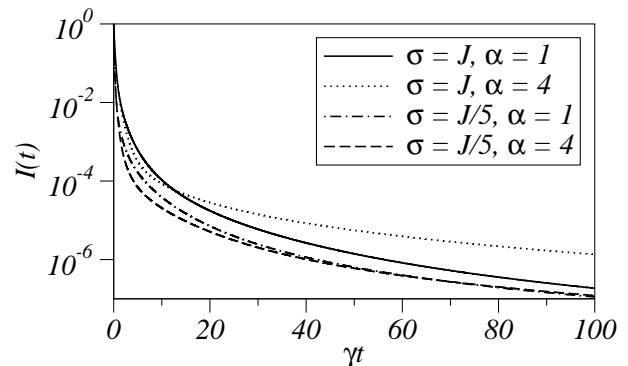


FIG. 2: Time dependence of the fluorescence decay after pulse excitation in weakly ($\alpha = 1$) and strongly ($\alpha = 4$) correlated 1D lattices when $U = 0$, for two different magnitudes of disorder. Lattice size is $N = 250$ and the results comprise the average over 200 realizations of the disorder.

V. BIASED SYSTEM

In disorder-free systems, switching the bias on results in a reorganization of the level structure, which becomes

equally spaced with level spacing U .¹³ The corresponding eigenstates become localized within a localization segment of length $L_U = W/U$ in units of the spatial period, where W is the bandwidth. In 1D disorder-free systems this bandwidth is $W = 4J$. This structure is revealed in photoluminescence^{21,22} and photoconductivity²³ spectra as a series of equally spaced peaks. Deviations from perfect periodicity broadens the peaks and makes them unresolved when disorder is uncorrelated and large. As mentioned in the Introduction, long-range correlations facilitate the occurrence of the WSL even if disorder is large.¹⁴ In this case, a periodic pattern is found to build up at the center of the optical absorption band, where the absorption spectrum lineshape is obtained from

$$A(E) = \frac{1}{N} \left\langle \sum_{\mu=1}^N f_{\mu} \delta(E - E_{\mu}) \right\rangle. \quad (7)$$

The period of the periodic pattern is equal to U , as for the WSL in an ideal lattice, and independent of the system size N . This pattern was attributed to the Wannier-Stark quantization of the energy spectrum in the long-range correlated disordered lattice.¹⁴

In Fig. 3 we plotted the absorption spectra calculated for disordered biased chains of $N = 250$ sites, choosing the magnitude of disorder $\sigma = J$ and the bias magnitude $U = 0.05J$. Averages over 10^6 realizations of disorder were performed in Eq. (7). Two values of the correlation exponents were considered, $\alpha = 1$ and $\alpha = 4$. The spectra broaden as compared to those of the unbiased systems (not shown in the figure). In Ref. 14 we proved that the spectrum broadens when $\sigma^* < UN$, namely when the absorption line width σ^* in the unbiased system is smaller than the potential energy drop across the entire lattice UN . The width of the absorption spectrum (FWHM) when U is low is of the order of $UN = 12.5$, as it is already observed in Fig. 3. However, the absorption spectra are still featureless and no signatures of the WSL are detected. The corresponding fluorescence decay is shown in Fig. 4, where we observe that the decay is non-exponential. At large time the decay is slower on increasing the magnitude of the correlation, similarly to what was found in the absence of bias (see Fig. 2).

In Fig. 5 we plotted the absorption spectra calculated for a high value of the bias, $U = 0.5J$. We observe in the upper panel that at $\alpha < \alpha_c$ the spectrum remains structureless. However, in the lower panel we see that for strong correlations in disorder, when $\alpha > \alpha_c$, the spectrum presents a periodic pattern which is not masked by the stochastic disorder fluctuations (see the inset in the lower panel). Most important, the period of the modulation is exactly equal to $U = 0.5J$, as results from the occurrence of the WSL in the energy spectrum of the system.

As mentioned above, long-range correlations in disorder strongly affect the optical response of the system. We now present evidences that they also have remarkable impact on the fluorescence decay. More important, we will

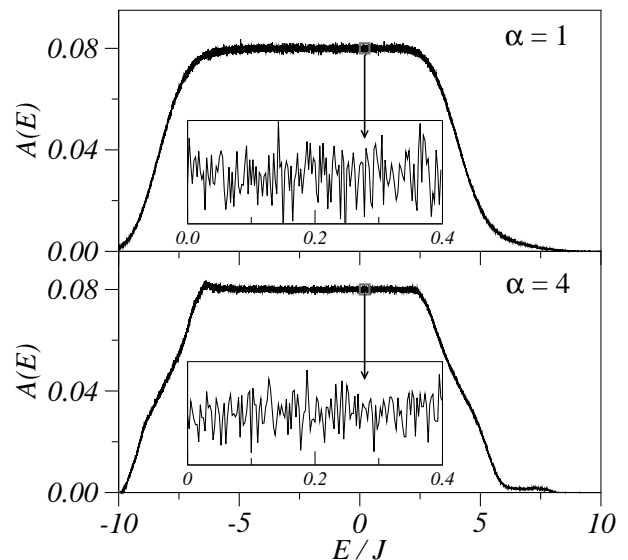


FIG. 3: Absorption spectra of biased chains ($U = 0.05J$) with $N = 250$ sites calculated for two values of the correlation exponent α , shown in the plot. The magnitude of disorder is $\sigma = J$. Each curve were obtained after averaging over 10^6 realizations of disorder. Insets show enlarged views of the spectra within the small boxes.

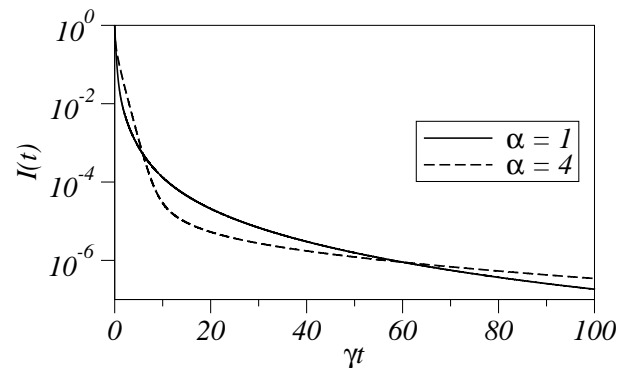


FIG. 4: Time dependence of the fluorescence decay after pulse excitation in weakly ($\alpha = 1$) and strongly ($\alpha = 4$) correlated 1D lattices when $U = 0.05J$ and $\sigma = J$. Lattice size is $N = 250$ and the results comprises the average over 200 realizations of the disorder.

show that the peculiarities found in the fluorescence decay can be related to the occurrence of the WSL. To this end, we numerically solve (2) and (5) to obtain the time-dependence of the fluorescence when $U \neq 0$. Figure 6 shows the fluorescence decay after pulse excitation as a function of γt for various set parameters and $W_0 = \gamma$. The lattice size is $N = 250$, the bias is $U = 0.5J$ and the results comprises the average over 200 realizations of the disorder. We observe that the fluorescence decay is still non-exponential when $\alpha < \alpha_c$. However, the decay is exponential in the opposite limit, when $\alpha > \alpha_c$. It is to be noticed that the system size N should be sufficiently large enough to yield the power-law spectral den-

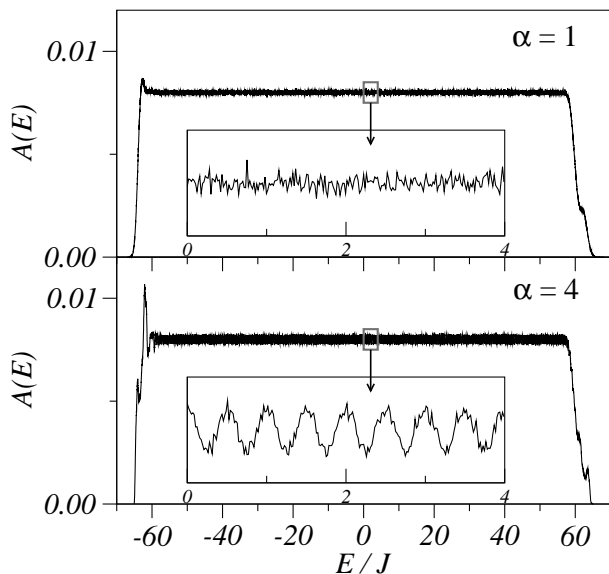


FIG. 5: Absorption spectra of biased chains ($U = 0.5J$) with $N = 250$ sites calculated for two values of the correlation exponent α , shown in the plot. The magnitude of disorder is $\sigma = J$. Each curve were obtained after averaging over 10^6 realizations of disorder. Insets show enlarged views of the spectra within the small boxes.

sity $S(k) \propto k^{-\alpha}$. If N is inadequately small, $S(k)$ would not obey a power law. To ascertain whether results mentioned above can be attributed to long-range spatial correlations, we also studied larger system sizes. Figure 6 also shows the fluorescence decay when $N = 1000$, the results comprising the average over 50 realizations of the disorder. The non-exponential and exponential decays for weakly and strongly correlated disorder respectively are clearly observed (see Sec. VI below for a detailed discussion of finite-size effects).

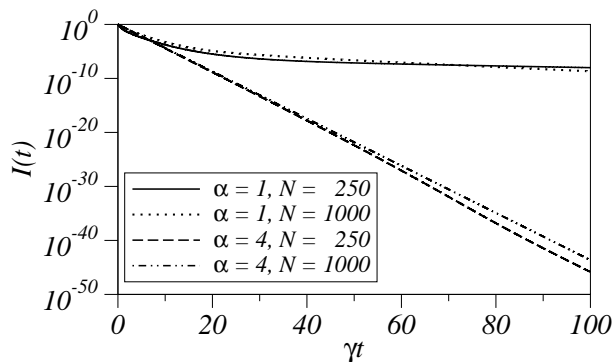


FIG. 6: Time dependence of the fluorescence decay after pulse excitation in weakly ($\alpha = 1$) and strongly ($\alpha = 4$) correlated 1D lattices when $U = 0.5J$ and $\sigma = J$. Lattice size is $N = 250$ and the results comprises the average over 200 realizations of the disorder. For comparison, results for larger systems ($N = 1000$) are also shown, comprising averages over 50 realizations of the disorder.

In Ref. 14 we claimed that the WSL can be resolved even if correlations are weak. We pointed out that the condition for the WSL to appear in the absorption spectrum is $\sigma > \sqrt{UJ}$ in the weakly correlated case. We calculated the absorption spectrum lineshape for magnitudes of disorder $\sigma = 0.2J$ and bias $U = 0.5J$, when this inequality holds. The results, obtained for $\alpha = 1$ and $\alpha = 4$ are depicted in Fig. 7 (upper and lower panels, respectively). One observes that the absorption spectrum shows a resolved WSL structure for both values of α . Figure 8 indicates that the fluorescence decay exponentially with time when $\alpha > \alpha_c$ and biexponentially when $\alpha < \alpha_c$.

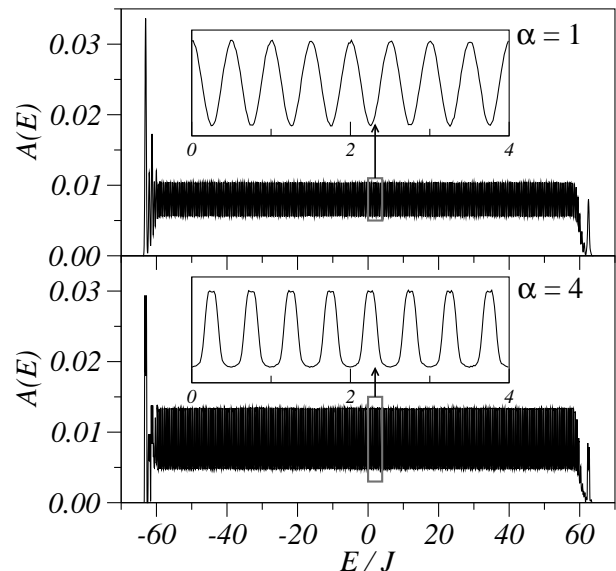


FIG. 7: Absorption spectra of biased chains ($U = 0.5J$) with $N = 250$ sites calculated for two values of the correlation exponent α , shown in the plot. The magnitude of disorder is $\sigma = 0.2J$. Each curve were obtained after averaging over 10^6 realizations of disorder. Insets show enlarged views of the spectra within the small boxes.

Results shown in Figs. 6 and 8 provide compelling evidences that the occurrence of the WSL in the energy spectrum may result in an exponential decay of the fluorescence. In the upper panel of Fig. 5 we observed the absence of WSL signatures in the optical absorption spectrum when $\alpha < \alpha_c$ and the magnitude of disorder σ is large. Simultaneously, the fluorescence decay is non-exponential, as shown in Fig. 6 and Fig. 8. This behavior can be understood from the fact that when σ is large and correlations are weak ($\alpha < \alpha_c$) the oscillator strength depends on the energy state, similarly to what it is found in the absence of bias (see Sec. IV). This finally leads to a non-exponential decay of the fluorescence. However, when correlations are strong, $\alpha \geq \alpha_c$, or the magnitude of disorder σ is smaller than \sqrt{UJ} , the occurrence of the WSL ladder is accompanied by an exponential decay of the fluorescence, as shown if Fig. 6. In this case localization by the bias U prevails over localization by disorder.

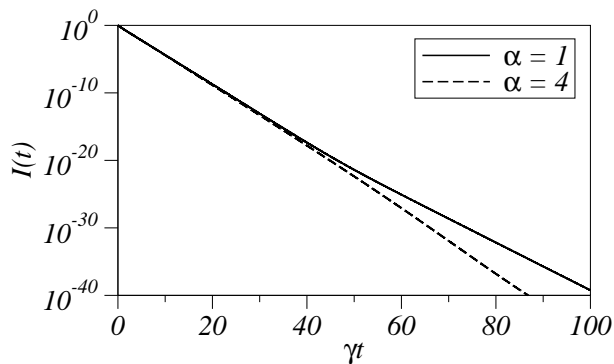


FIG. 8: Time dependence of the fluorescence decay after pulse excitation in weakly ($\alpha = 1$) and strongly ($\alpha = 4$) correlated 1D lattices when $U = 0.5J$ and $\sigma = 0.2J$. Lattice size is $N = 250$ and the results comprises the average over 200 realizations of the disorder.

When the WSL arises, the shape of the eigenfunction is almost the same for all states, except for a trivial space shift and excluding finite size effects (see Fig. 9). Consequently, the oscillator strength of all states has the same value, yielding a single exponential in the decay law of the fluorescence.

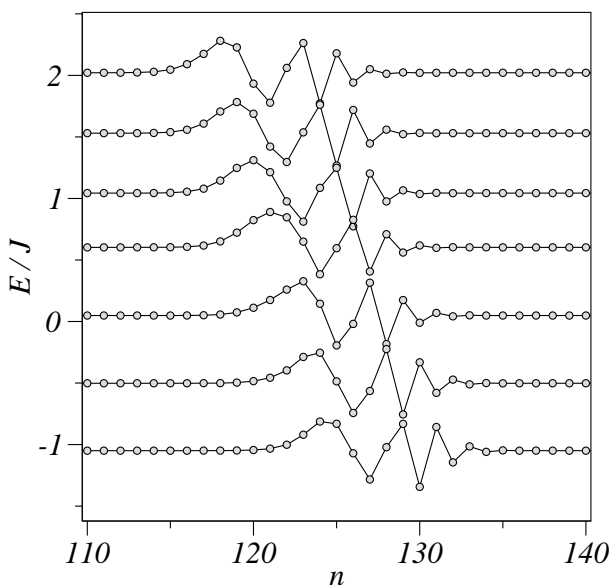


FIG. 9: A subset of eigenstates for a typical realization of the random energy potential when $U = 0.5$ for a lattice of size $N = 250$, magnitude of disorder $\sigma = 0.2J$, and correlation exponent $\alpha = 1$. The baseline indicates the energy of the eigenstate.

VI. FINITE SIZE EFFECTS

The peculiarities observed at the low- and high-energy sides of the absorption spectra shown in Figs. 5 and 7 are

associated with finite size effects.¹⁴ The levels of these regions of the energy spectrum are formed by the states localized close to the system ends. Because of that, the corresponding eigenfunctions differ from those at the band center. As a consequence, not all eigenstates present exactly the same value of the oscillator strength and slight deviation from the single exponential decay of the fluorescence can be detected.

To understand the relevance of finite size effects, we focus on the biased, disorder-free lattice. In the thermodynamic limit ($N \rightarrow \infty$), the normalized eigenstates of the Hamiltonian (2) with $\sigma = 0$ are expressed in terms of the Bessel functions as $\psi_{\mu,n} = J_{n-\mu}(2J/U)$ (see Ref. 24). The corresponding eigenenergies are $E_{\mu} = \mu U$, μ being an integer (i.e. the WSL structure). The oscillator strength can also be calculated exactly in this limiting case $f_{\mu} = 1$, which takes the same value for all states, as expected. Remarkably, the oscillator strength becomes also independent of the bias U in large disorder-free systems. From (6) we conclude that the normalized fluorescence intensity is nothing but the survival probability $I(t) = \sum_{\mu=1}^N P_{\mu}(t)$ in this case. Summing over all states in (5) we obtain $\dot{I}(t) = -\gamma I(t)$, leading to $I(t) = \exp(-\gamma t)$. Consequently, the fluorescence decay in biased disorder-free lattices is the same as in the isolated monomer (i.e. single exponential with decay time $1/\gamma$), when the system is large enough.

As mentioned in the preceding paragraph, when $N \rightarrow \infty$ the occurrence of the WSL in the energy spectrum ($E_{\mu} = \mu U$) in disorder-free systems leads to an exponential decay of the fluorescence. The decay time is found to be the same as in the single monomer and consequently it is independent of the bias. We have performed simulations in finite system when $\sigma = 0$ to obtain the decay time τ_{∞} from the fluorescence intensity curves when $t \rightarrow \infty$. Results are shown in Fig. 10, where we observe that $\gamma\tau_{\infty}$ approaches the theoretical limit ($\gamma\tau_{\infty} = 1$) on increasing both the system size or the bias. The localization length L_U due to the presence of the bias decreases on increasing U , leading to smaller finite size effects.

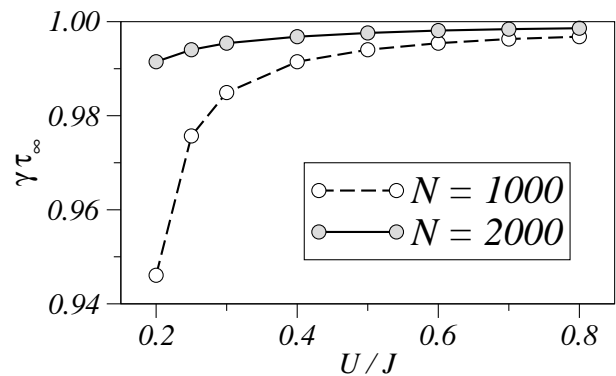


FIG. 10: Bias dependence of $\gamma\tau_{\infty}$ for different system sizes, when $\sigma = 0$.

Finite size effects are also relevant in a biased lattice

with long-range correlated disorder. In Fig. 11 we observe a similar trend to that found in disorder-free lattices. The main difference is related to the value of τ_∞ , which is slightly lower than in disorder-free lattices of the same size.

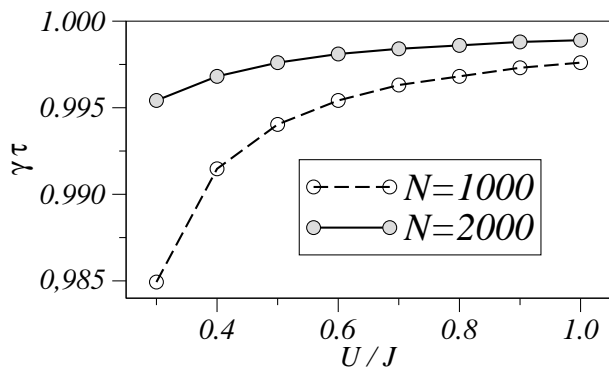


FIG. 11: Bias dependence of $\gamma\tau_\infty$ for different system sizes, when $\sigma = J$ and $\alpha = 4$. Results comprise averages over 50 realizations of disorder.

VII. CONCLUSIONS

We studied numerically the intraband exciton relaxation in a 1D disordered lattice subjected to a linear bias of magnitude U . The random site potential presents a power-law spectral density $S(k) \sim 1/k^\alpha$, which gives rise to long-range correlations in site energies. Exciton transport is considered as incoherent hoppings over the eigenstates of the static lattice, arising when the coupling to vibrations is taken into account. The dynamics of the intraband relaxation is monitored by means of the fluorescence decay after broadband pulse excitation.

Fluorescence decay in the unbiased lattice ($U = 0$) was found to be non-exponential in both weakly ($\alpha < \alpha_c = 2$)

and strongly ($\alpha > \alpha_c = 2$) correlations limits. This time dependence reflects the existence of many decay channels in the system with different decay times. In other words, the wave functions vary from state to state and consequently the distribution of the oscillator strengths is rather broad. We found a slowdown of the fluorescence decay when $\alpha > \alpha_c$, which we relate to the peculiar level structure of level in this case: there exist dark states below those states with high oscillator strength located deep in the band (like that labeled 3 in Fig. 1).

At moderate bias the absorption spectrum broadens as compared to the unbiased case, but no signatures of the WSL are found. The structureless spectrum is accompanied by a non-exponential decay of the fluorescence. However, on further increasing the magnitude of the bias, a periodic pattern is found to build up at the center of the (already wide) absorption band when $\alpha > \alpha_c$. Its period is equal to U , as for the WSL in an ideal lattice, and independent of the system size N . Simultaneously, the fluorescence decay is described approximately by a single exponential. Finally, when the parameter \sqrt{UJ} exceeds the magnitude of disorder σ , the WSL in the absorption spectrum and the exponential decay of the fluorescence appear, irrespective of the value of the correlation exponent α . The single exponential decay of the fluorescence is a direct consequence of the localization by the bias, since all states carries approximately the same value of the oscillator strength. Deviations from perfect exponential decay were related not only to stochastic fluctuations of the disorder but mainly to finite size effects.

Acknowledgments

The authors thank V. A. Malyshev for helpful conversations. This work was supported by MEC (Project MOSAICO).

¹ M. Paczuski, S. Maslov, and P. Bak, Phys. Rev. E **53**, 414 (1996).
² S. Havlin, S. V. Buldyrev, A. Bunde, A. L. Goldberger, P. Ch. Ivanov, C.-K. Peng, and H. E. Stanley, Physica A **273**, 46 (1999).
³ P. Carpena, P. Bernaola-Galván, P. Ch. Ivanov, and H. E. Stanley, Nature **418**, 955 (2002); *ibid* **421**, 764 (2003).
⁴ H. Yamada, Phys. Lett. A **332**, 65 (2004); Int. J. Mod. Phys. B **18**, 1697 (2004); Phys. Rev. B **69**, 014205 (2004).
⁵ E. L. Albuquerque, M. S. Vasconcelos, M. L. Lyra, and F. A. B. F. de Moura, Phys. Rev. E, **71**, 021910 (2005).
⁶ S. Roche, D. Bicoût, and E. Maciá, Phys. Rev. Lett. B **91**, 109901 (2004).
⁷ F. A. B. F. de Moura and M. L. Lyra, Phys. Rev. Lett. **81**, 3735 (1998).
⁸ F. M. Izrailev and A. A. Krokhin, Phys. Rev. Lett. **82**, 4062 (1999).

⁹ G.-P. Zhang and S.-J. Xiong, Eur. Phys. J. B **29**, 491 (2002).
¹⁰ H. Shima, T. Nomura, and T. Nakayama, Phys. Rev. B **70**, 075116 (2004).
¹¹ F. Bloch, Z. Phys. **52**, 555 (1928).
¹² F. Domínguez-Adame, V. A. Malyshev, F. A. B. F. de Moura, and M. L. Lyra, Phys. Rev. Lett. **91**, 197402 (2003).
¹³ G. H. Wannier, Phys. Rev. **117**, 432 (1960).
¹⁴ E. Díaz, F. Domínguez-Adame, Yu. A. Kosevich, and V. A. Malyshev, Phys. Rev. B **73**, 172410 (2006).
¹⁵ D. J. Heijs, V. M. Malyshev, and J. Knoester, J. Chem. Phys. **121**, 4884 (2004).
¹⁶ M. Bernarz, V. A. Malyshev, and J. Knoester, J. Chem. Phys. **117**, 6200 (2002).
¹⁷ M. Shimizu, S. Suto, and T. Goto, J. Chem. Phys. **114**, 2775 (2001).

- ¹⁸ M. Bednarz, V. A. Malyshev, J. P. Lemaistre, and J. Knoester, *J. Lumin.* **94-95**, 271 (2001).
- ¹⁹ A. V. Malyshev, V. A. Malyshev, and F. Domínguez-Adame, *Chem. Phys. Lett.* **371**, 417 (2003).
- ²⁰ A. V. Malyshev, V. A. Malyshev, and F. Domínguez-Adame, *J. Phys. Chem.* **107**, 4418 (2003).
- ²¹ E. E. Méndez, F. Agulló-Rueda, and J. M. Hong, *Phys. Rev. Lett.* **60**, 2426 (1988).
- ²² F. Agulló-Rueda, E. E. Méndez, and J. M. Hong, *Phys. Rev. B* **40**, 1357 (1989).
- ²³ M. K. Saker, D. M. Whitteker, M. S. Skolnick, M. T. Emeny, and C. R. Whitehouse, *Phys. Rev. B* **43**, 4945 (1991).
- ²⁴ H. Fukuyama, R. A. Bari, and H. C. Fogedby, *Phys. Rev. B* **8**, 5579 (1973).